Chemical Engineering Journal 204–206 (2012) 179–187

Contents lists available at SciVerse ScienceDirect

Chemical Engineering Journal

journal homepage: www.elsevier.com/locate/cej

Consideration of a target product concentration level in the optimal design of a four-zone simulated moving bed process for binary separation

Sungyong Mun *

Department of Chemical Engineering, Hanyang University, Haengdang-dong, Seongdong-gu, Seoul 133-791, South Korea

HIGHLIGHTS

- The constraint on product concentration was considered in linear SMB optimizations.
- The factors affecting SMB product concentration were clarified with SWD method.
- Column length played an important role in the aforementioned optimization.
- Column configuration had a large effect on throughput and product concentration.
- Linear SMBs with a target product concentration level were successfully optimized.

ARTICLE INFO

Article history:
Received 23 May 2012
Received in revised form 10 July 2012
Accepted 11 July 2012
Available online 22 July 2012

Keywords:
Simulated moving bed
Product concentration
Standing wave design

ABSTRACT

In the stage of optimizing a simulated moving bed (SMB) process for continuous separation, the extent of product concentration can sometimes be as important as the other performance criteria such as throughput and product purities. In such cases, the issue of maintaining the product concentration higher than a given target level needs to be taken into account during the SMB optimization. To investigate this issue, the throughput of an SMB process for binary separation was optimized in this study using a model separation system while placing a constraint on product concentration as well as pressure drop. The resultant throughput from such SMB optimization was highly affected by column length. It was found first that the throughput was limited by the constraint on the product concentration in the region of short columns but limited by the constraint on the pressure drop in the region of long columns. As a result, the optimal column length leading to the highest throughput occurred at the boundary between the product-concentration limiting region and the pressure-drop limiting region. In addition to the column length, the column configuration also played an important role in the optimization of the SMB with the constraint on the product concentration. As the target level of the raffinate product concentration was set higher, the optimal column configuration leading to the maximum throughput showed the pattern of placing more columns in zone IV. By contrast, the placement of more columns in zone I became the pattern of optimal column configuration when the target level of the extract product concentration was set higher. The results and methodology in this article will be useful when there is a necessity for developing SMBs that are to meet a certain requirement imposed on product concentration.

1. Introduction

Simulated moving bed (SMB) chromatography has been recognized as one of highly efficient processes for continuous separation of petrochemicals, sugars, biochemicals, chiral drugs, or pharmaceuticals [1–4]. This process generally consists of multiple chromatographic columns packed with a proper adsorbent, which are partitioned into four zones by the locations of two inlet (feed and desorbent) and two outlet (raffinate and extract) ports as illustrated in Fig. 1. To enable the continuous loading of a feed mixture and the continuous collection of product streams at the same time, the four ports are set to move periodically in the direction of liquid flow at a predetermined time interval (or switching time). It has been confirmed that such an SMB chromatographic process surpasses a conventional batch chromatography to a remarkable extent in the aspects of throughput and product purities [1–6]. This has led the SMB process to be widely accepted as a large-scale separation process that needs high economical efficiency, high production rate, and stringent purity requirement.

However, only the aforementioned throughput and product purities cannot represent the overall performance criteria of SMB

* Tel.: +82 2 2220 0483; fax: +82 2 2298 4101.
E-mail address: munsy@hanyang.ac.kr

1385-8947/$ - see front matter © 2012 Elsevier B.V. All rights reserved.
http://dx.doi.org/10.1016/j.cej.2012.07.074

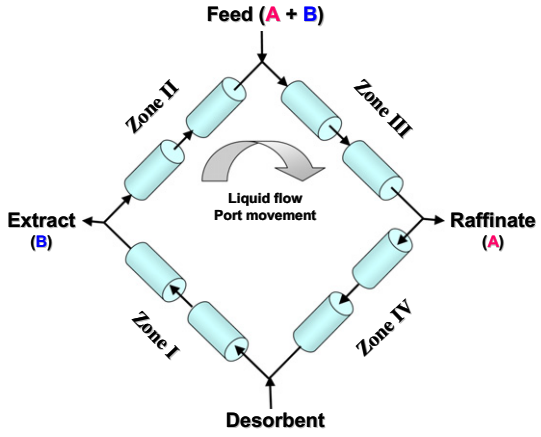

Fig. 1. Schematic diagram of a four-zone SMB process for binary separation. (A) Low-affinity solute (or fast-migrating solute), (B) high-affinity solute (or slow-migrating solute).

process. In some cases, the product concentration can become an important issue, which will happen particularly when (1) the product stream from SMB needs to be treated again by the subsequent crystallization step and (2) the efficiency of the crystallization step or the quality of its output is largely affected by the extent of its feed concentration, i.e. the extent of the product concentration of the preceding SMB process [7]. Thus, in such cases, a target level of product concentration needs to be taken into account in the stage of SMB optimization. In other words, the SMB optimization should be carried out in such a way that either the highest throughout or the highest purities can be attained while meeting the required constraint on the product concentration. However, in most of previous SMB optimization studies in the literature, the issue of maintaining the required level of product concentration has not been taken into account.

The aforementioned issue will be handled in this study for the first time. For this study, the mixture of two amino acids, phenylalanine and tyrosine [8], will be utilized as a model separation system and the standing wave design (SWD) method [2–4,9–12] will be adopted as a major frame for SMB optimization. First, the throughput of the SMB process for separation of the model system will be optimized under the constraint that the product concentration should be maintained higher than a given target level. The results from these optimizations will then be used to investigate how the SMB throughput is affected by the constraint on the product concentration. Furthermore, the major factors related to the extent of SMB product concentration will be clarified using the SWD equations, followed by being verified with the results from the optimizations for the SMB of interest. Finally, it will be studied how the magnitude of the target level of product concentration influences the throughput, column length, and column configuration of the optimized SMB process.

2. Theory

2.1. Standing wave design (SWD) method for the optimal design of a four-zone SMB for binary separation

In the stage of developing an SMB process for a new separation task, it is of the utmost importance to obtain its optimal operation parameters that can guarantee the highest throughput while meeting the required product purities. In regard to this issue, several relevant methods have been developed in the literature [9–18]. Among them, the standing wave design (SWD) method was reported to be highly effective in the optimal determination of SMB operation parameters [2–4,9–12], particularly in the case of low-pressure SMB systems where a considerable extent of mass-transfer resistance is always present due to the use of a relatively large adsorbent particle size.

The effectiveness of such SWD method has been validated theoretically and experimentally in many of previous studies [2–4,9–12]. Furthermore, it is known that the SWD can easily be upgraded into more comprehensive optimization tool with various constraints and objectives while allowing the reflection of any particular considerations for a given separation task. For these reasons, the SWD was chosen in this study as a key frame in optimizing the SMB process with the constraint that the product concentration should be maintained higher than a given target level.

The core principle of the aforementioned SWD is to select the SMB operation parameters (four zone flow rates and switching time) in such a way that each key concentration wave can be made standing in its respective zone on the time-averaged sense [2–4,9–12]. To realize this principle, the migration velocity of a key concentration wave in each zone should be matched with the port movement velocity. The relevant SWD equations leading to such a standing-wave condition in a four-zone SMB process have been established previously for linear isotherm systems [9,11], and they are summarized below for the ideal case where there is no axial dispersion and mass-transfer resistance.

$$Q^{\mathrm{I}} = S[\varepsilon_b + (1-\varepsilon_b)\delta_{\mathrm{B}}]v \tag{1a}$$

$$Q^{\mathrm{II}} = S[\varepsilon_b + (1-\varepsilon_b)\delta_{\mathrm{A}}]v \tag{1b}$$

$$Q^{\mathrm{III}} = S[\varepsilon_b + (1-\varepsilon_b)\delta_{\mathrm{B}}]v \tag{1c}$$

$$Q^{\mathrm{IV}} = S[\varepsilon_b + (1-\varepsilon_b)\delta_{\mathrm{A}}]v \tag{1d}$$

where the superscripts I to IV stand for zone number; the subscripts A and B indicate the low-affinity (or fast-migrating) and the high-affinity (or slow-migrating) components respectively; Q^j is the volumetric flow rate in zone j; S is the cross-sectional area of each column; ε_b is the inter-particle porosity; v is the average port velocity; and δ_i is the retention factor of component i that is defined as $\varepsilon_p + (1-\varepsilon_p)a_i$, where ε_p is the intra-particle porosity and a_i is the linear isotherm parameter of component i.

The aforementioned SWD equations, however, are inappropriate for the actual SMB optimization because axial dispersion and mass-transfer resistance become a matter of grave concern in realistic SMB systems. To counter the wave spreading due to such mass-transfer effects, the aforementioned SWD equations should be modified to include a proper mass-transfer correction term as follows [2–4,9–12].

$$Q^{\mathrm{I}} = S[\varepsilon_b + (1-\varepsilon_b)\delta_{\mathrm{B}}]v + \Delta_{\mathrm{B}}^{\mathrm{I}} \tag{2a}$$

$$Q^{\mathrm{II}} = S[\varepsilon_b + (1-\varepsilon_b)\delta_{\mathrm{A}}]v + \Delta_{\mathrm{A}}^{\mathrm{II}} \tag{2b}$$

$$Q^{\mathrm{III}} = S[\varepsilon_b + (1-\varepsilon_b)\delta_{\mathrm{B}}]v - \Delta_{\mathrm{B}}^{\mathrm{III}} \tag{2c}$$

$$Q^{\mathrm{IV}} = S[\varepsilon_b + (1-\varepsilon_b)\delta_{\mathrm{A}}]v - \Delta_{\mathrm{A}}^{\mathrm{IV}} \tag{2d}$$

where Δ_i^j is the mass-transfer correction term of component i in zone j and it is given by [2–4,9–12]

$$\Delta_i^j = \frac{\varepsilon_b S \beta_i^j}{N^j L_c}\left[E_{b,i}^j + \frac{(1-\varepsilon_b)(\delta_i v)^2}{\varepsilon_b K_{f,i}^j}\right] \tag{3}$$

where N^j is the number of columns in zone j; L_c is the length of each column; E_b is the axial dispersion coefficient; and β is an index of product purity and yield; the larger the β value, the higher the

product purity and yield [9–12]. The lumped mass-transfer coefficient (K_f) can be estimated from the following equation [9–12]:

$$\frac{1}{K_f} = \frac{R^2}{15K_e\varepsilon_p D_p} + \frac{R}{3k_f} \tag{4}$$

where R is the radius of adsorbent particle; D_p is the intra-particle diffusivity; and k_f is the film mass-transfer coefficient. It was reported that the operation parameters resulting from the above SWD equations enables the relevant SMB process to obtain the highest throughput and the lowest desorbent consumption while guaranteeing that desired product yields and purities can be maintained [2–4,9–12].

2.2. Use of the SWD equations for clarification of the factors affecting the product concentration

To clarify the key factors affecting the concentration of a product stream from SMB, one can derive the following two dimensionless concentrations ($\overline{C}_{raf,A}$ and $\overline{C}_{ext,B}$) from the SWD equations as follows.

$$\overline{C}_{raf,A} \equiv \frac{C_{raf,A}}{C_{feed,A}} = Y_A\left(\frac{\psi - \Delta_A^{II}}{\psi + \Delta_A^{IV}}\right) \tag{5}$$

$$\overline{C}_{ext,B} \equiv \frac{C_{ext,B}}{C_{feed,B}} = Y_B\left(\frac{\lambda - \Delta_B^{III}}{\lambda + \Delta_B^{I}}\right) \tag{6}$$

where $\psi = S(1-\varepsilon_b)(\delta_B - \delta_A)v - \Delta_B^{III}$ and $\lambda = S(1-\varepsilon_b)(\delta_B - \delta_A)v - \Delta_A^{II}$. In addition, $C_{raf,A}$ and $C_{ext,B}$ indicate the product concentrations of a raffinate component (A) and an extract component (B) respectively; $C_{feed,A}$ and $C_{feed,B}$ are the feed concentrations of a raffinate component (A) and a extract component (B) respectively; and Y_A and Y_B are the product yields of a raffinate component (A) and an extract component (B) respectively. The derivation procedures for the above two equations are presented in Appendix A.

It is clear from the above expressions that both $\overline{C}_{raf,A}$ and $\overline{C}_{ext,B}$ are less than unity, which means that the dilution of the raffinate and extract products is inevitable. Therefore, the highest product concentration obtainable is virtually equal to the feed concentration, which happens when $\Delta_A^{II} = \Delta_A^{IV} = 0$ and $Y_A = 1$ for the raffinate product concentration and $\Delta_B^{I} = \Delta_B^{III} = 0$ and $Y_B = 1$ for the extract product concentration.

One of the noteworthy points in the expression for $\overline{C}_{raf,A}$ is that it is highly affected by Δ_A^{II} and Δ_A^{IV}. It is evident from Eq. (5) that as Δ_A^{II} and Δ_A^{IV} are reduced, $\overline{C}_{raf,A}$ increases, i.e. the raffinate product is less diluted. Thus, the Δ_A^{II} and Δ_A^{IV} will be called hereafter as the *RD*-factors, which signify the factors affecting the dilution of the raffinate product. Between these two *RD*-factors, it can be inferred that Δ_A^{IV} can have more significant impact on the raffinate dilution than Δ_A^{II}, because Δ_A^{IV} is located in the denominator of the equation for $\overline{C}_{raf,A}$ while Δ_A^{II} in the numerator.

Similarly, it can readily be grasped in the expression for $\overline{C}_{ext,B}$ that it is highly affected by Δ_B^{I} and Δ_B^{III}. Its relevant equation also reveals that a reduction in Δ_B^{I} and Δ_B^{III} leads to an increase in $\overline{C}_{ext,B}$, i.e. less dilution of the extract product. Thus, the Δ_B^{I} and Δ_B^{III} will be called hereafter as the *ED*-factors, which signify the factors affecting the dilution of the extract product. Between these two *ED*-factors, Δ_B^{I} will have a larger influence on the extract dilution than Δ_B^{III} for the same reason as above.The mathematical expressions for the *RD*-factors (Δ_A^{II}, Δ_A^{IV}) and the *ED*-factors (Δ_B^{I}, Δ_B^{III}) can be discerned by substituting the relevant zone number and component identity for the superscript j and the subscript i in Eq. (3). The resulting expressions for such two factors clearly show that they are largely dependent on the column length (L_c), the port velocity (v), and the number of columns in zone j (N^j), i.e. the column configuration. It is clear first from Eq. (3) that the use of a larger L_c can reduce the *RD*-factors and *ED*-factors, thereby increasing both product concentrations. It is also evident that the *RD*-factors and *ED*-factors can be reduced simultaneously by decreasing v. It is known that such a decrease in v is usually caused by decreasing the feed flow rate of SMB process [9,11]. In regard to the column configuration (N^j), it can readily be grasped from Eq. (3) that the increase of the column numbers in zones II and IV can be effective in reducing the *RD*-factors while the increase of the column numbers in zones I and III can be effective in reducing the *ED*-factors.

3. Approach

3.1. Formulation of the optimization problems

3.1.1. Case I: maximization of throughput under the constraint on product concentration while fixing the column configuration at 2–2–2–2

In the first type of optimization problem (Case I), the SMB process was optimized to maximize throughput under the constraint on product concentration while fixing the column configuration at 2–2–2–2. The objective function employed in this optimization is the throughput, which is defined as follows:

$$\text{Throughput} = \frac{Q_{feed}}{BV} = \frac{4Q_{feed}}{N_{tot}\pi d_c^2 L_c} \tag{7}$$

where Q_{feed} is the feed flow rate; BV is the total bed volume; N_{tot} is the total column number; and d_c is the column diameter.

During the aforementioned Case I optimization, the purities of both extract and raffinate products were set at 98% and the pressure drop over the SMB unit was constrained to be maintained below 100 psi, which corresponds to a general criterion for low-pressure chromatographic processes in bioproduct industry [4,10]. The other details in such an optimization task are presented in the following optimization frame.

$$\text{Max} \quad J = \text{Throughput}\left[Q^I, Q^{II}, Q^{III}, t_s\right] \tag{8a}$$

$$\text{Subject to} \quad PurA = 98\%,\ PurB = 98\% \tag{8b}$$

$$C_{prod,i}/C_{feed,i} \geqslant \alpha$$

$$\Delta P \leqslant 100 \text{ psi}$$

$$\text{Dependent variables} \quad Q_{feed} = Q^{III} - Q^{II} \tag{8c}$$

$$Q_{des} = Q^{I} - Q^{IV} \tag{8d}$$

$$Q_{ext} = Q^{I} - Q^{II} \tag{8e}$$

$$Q_{raf} = Q^{III} - Q^{IV} \tag{8f}$$

$$\text{Fixed variables} \quad \chi = 2{-}2{-}2{-}2 \tag{8g}$$

$$N_{tot} = 8 \tag{8h}$$

where *PurA* and *PurB* are the purities of raffinate product (A) and extract product (B) respectively; α is the target level of product concentration; and χ stands for the column configuration. In addition, ΔP is the pressured drop over the SMB unit, which is generally expressed as the summation of the pressure drop occurring in each zone as follows [3,10,12]:

$$\Delta P = \Delta P^{I} + \Delta P^{II} + \Delta P^{III} + \Delta P^{IV} \tag{9}$$

where ΔP^j is the pressure drop through zone j and it is usually estimated from the Ergun equation [19].

To reduce the computation time for the above optimization task, the column length was not directly included as one of the decision variables, as can be seen in Eq. (8a). Instead, the column length is changed in a discrete manner and for each step the five decision variables (Q^I, Q^{II}, Q^{III}, Q^{III}, t_s) are optimized on the basis of the SWD method. This approach can be of advantage to the

analysis of the optimization results, because the effect of the column length on throughput can be demonstrated while finding out the optimal column length.

3.1.2. Case II: maximization of throughput under the constraint on product concentration while including the column configuration as one of the decision variables

In the second type of optimization (Case II), the objective function and the constraints were kept the same as in the previous Case I optimization. The only difference was that only two columns were assigned to each zone in the Case I optimization whereas more than two columns were allowed to be placed in each zone in the Case II optimization. Furthermore, the number of columns in each zone, i.e. the column configuration (χ) was included as one of the decision variables in the Case II optimization, where the upper bound in the total column number (N_{tot}) was set at 20.

Therefore, if the results from the Case II optimization will be compared with those from the Case I optimization, it will be possible to clarify the effect of column configuration on the optimization of the SMB with the constraint on the product concentration.

3.2. Preparation of the SWD optimization tool for the SMB process with the requirement on a target level of the product concentration

Based on the above-mentioned optimization frame, the electronic program for optimizing the SMB with the requirement on a target level of product concentration was prepared using FORTRAN. Fig. 2 shows the overall algorithm of the prepared optimization program, which consists of one process box and three repetition loops such as innermost, inner, and outer loops. Among them, the process box performs the computation of the SWD equations (Eq. (2)), which plays a part in producing the optimal zone flow rates and the switching time for the given feed flow rate, column configuration, and column length. Such SWD computation is repeated while increasing the feed flow rate. This procedure lasts until the resultant operating parameters from the SWD are limited by either of the constraints imposed on product concentration and pressure drop. All of these executions are controlled by the innermost loop of the program (Fig. 2).

Each time the aforementioned innermost-loop executions are completed, the optimization program implements the inner-loop action, which is to vary the column configuration and then to activate the innermost-loop executions again under the varied column configuration. All the computations and executions above are repeated while varying the column length in the outer loop. During such a repetitive execution by the three loops in series, the operation parameters, column configuration, and column length leading to maximization of throughput can be obtained.

4. Results and discussion

The binary amino acid mixture, which was available in the literature [8], was chosen as a model separation system for investigating the issue of considering a target level of product concentration in the optimization of a four-zone SMB process. The linear isotherm and mass-transfer parameters of the two amino acid components comprising the feed mixture were reported in a previous study [8] and they are listed in Table 1 along with the

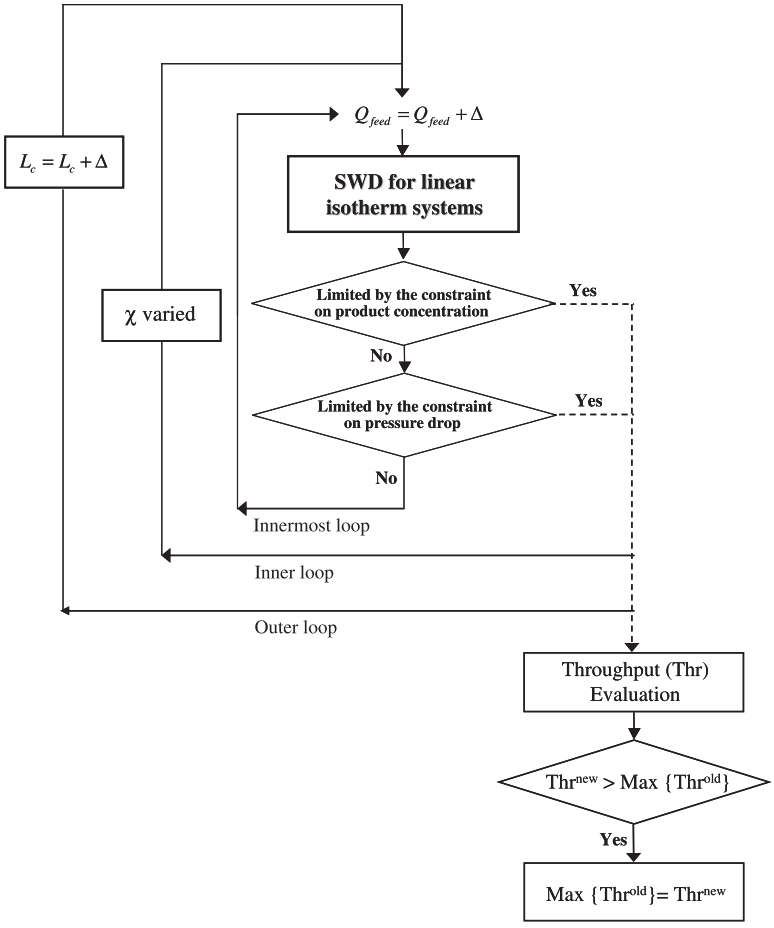

Fig. 2. The overall algorithm of the SWD optimization tool for the SMB process with the requirement on a target level of product concentration.

Table 1
System parameters and the other details of the binary-separation systems used in the optimization of a four-zone SMB process with the constraint on product concentration.

	Phenylalanine (A)	Tyrosine (B)
Linear isotherm parameter (a)	1.947	3.229
Molecular diffusivity (D_∞), cm^2/min	4.24×10^{-4}	4.12×10^{-4}
Intra-particle diffusivity (D_p), cm^2/min	1.02×10^{-4}	1.01×10^{-4}
Axial dispersion coefficient (E_b), cm^2/min	Chung and Wen correlation [20]	
Film mass-transfer coefficient (k_f), cm/min	Wilson and Geankoplis correlation [21]	
Adsorbent particle diameter (d_p), μm	100	
Column diameter (d_c), cm	2.5	
Inter-particle porosity (ε_b)	0.37	
Intra-particle porosity (ε_p)	0.55	

Data for a, D_∞, D_p, E_b, k_f, ε_b, and ε_p are from Ref. [8].

adsorbent particle size and column properties. As shown in Table 1, the two components such as phenylalanine and tyrosine have the lower and the higher adsorption-affinities respectively, and they follow a linear isotherm relationship. Therefore, in the four-zone SMB process of interest, phenylalanine (A) and tyrosine (B) will become a raffinate product and an extract product respectively.

4.1. Case I optimization with the constraint on the raffinate product concentration

The Case I optimization was carried out for the aforementioned four-zone SMB on the bases of the system parameters in Table 1 and the relevant optimization frames (Eq. (8)), which was aimed at maximizing the throughput of the SMB process with the column configuration of 2–2–2–2. The constraint taken into account in the first run of the Case I optimization was that the raffinate product concentration should always be higher than 90% of the feed concentration (i.e., $C_{raf,A}/C_{feed,A} \geqslant 0.9$). This task was repeated in series by varying the column length at the intervals of 1 cm and the results are presented in Fig. 3. It is clearly seen that the SMB throughput is largely affected by the column length (Fig. 3a). In the region of long columns (>46 cm), the throughput becomes lower as the column length increases. By contrast, in the region of short columns (<46 cm), the throughput decreases with decreasing the column length. As a consequence, a maximum in the throughput occurs at the column length of 46 cm, which virtually corresponds to the optimal column length for the SMB that is required to maintain the condition of $C_{raf,A}/C_{feed,A} \geqslant 0.9$ (Fig. 3a).

The aforementioned phenomenon occurs because the SMB column length influences pressure drop and product concentration simultaneously, which are both related to the key constraints for the process of interest. To check this point in more detail, the pressure drop of the optimized SMB at each column length was calculated from the Ergun equation [19]. The calculated pressure drops were then presented as a function of column length in Fig. 3b. Note that the pressure drop is always maintained at its upper limit (100 psi) when the column length is larger than 46 cm. This result indicates that the throughput of the SMB process with long columns (>46 cm) is virtually limited by the pressure-drop constraint. In such a pressure-limiting region, the increase of column length necessarily causes a reduction in the feed flow rate in order to prevent the excess of pressure drop beyond its upper limit (100 psi). Therefore, the throughput, if limited by the pressure drop, has a decreasing trend as the column length increases (Fig. 3b).

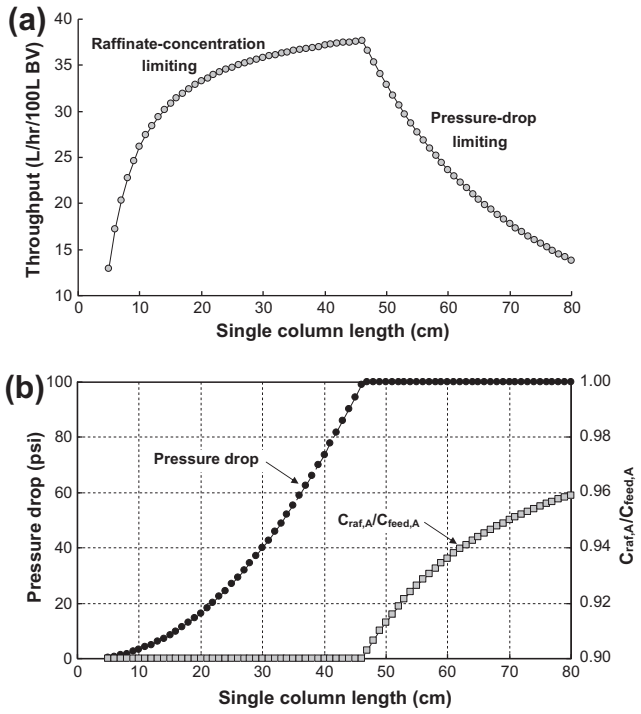

Fig. 3. Effect of single column length on the results from the Case I optimization with the constraint of $C_{raf,A}/C_{feed,A} \geqslant 0.9$. (a) Throughput, (b) $C_{raf,A}/C_{feed,A}$ and pressure drop.

By contrast, if the column length is smaller than 46 cm, the pressure drop of the corresponding SMB process is reduced to below 100 psi as shown in Fig. 3b. This means that in the region of short columns (<46 cm), the pressure drop can no longer be a limiting factor for the SMB throughput. To clarify the actual limiting factor for such case, the $C_{raf,A}/C_{feed,A}$ value of the optimized SMB at each column length was obtained from the SWD output. The resulting $C_{raf,A}/C_{feed,A}$ values were then plotted as a function of column length in Fig. 3b. We see that the $C_{raf,A}/C_{feed,A}$ value is always maintained at its lower limit (0.9) when the column length is smaller than 46 cm. This result indicates that the throughput of the SMB process with short columns (<46 cm) is virtually limited by the constraint imposed on the raffinate product concentration. In such a raffinate-concentration limiting region, the effect of column length on the SMB throughput can be interpreted by using the *RD*-factors ($\Delta_A^{II}, \Delta_A^{IV}$), which were mentioned in the theory section as the factors promoting the dilution of the raffinate stream.

According to the *RD*-factor expressions from the SWD (Eqs. (3) and (5)), a shorter column length leads to an increase in the *RD*-factors, resulting in a reduction in the raffinate product concentration. It is thus inferred that the decrease of column length in the region of short columns (<46 cm) in Fig. 3b can make the $C_{raf,A}/C_{feed,A}$ value drop below its lower limit. To prevent such a drop of the raffinate production concentration below its lower limit, a significant reduction in the feed flow rate is needed because it enables the *RD*-factors to become smaller by decreasing the port velocity (Eq. (3)). This is why the throughput, if limited by the constraint on the raffinate product concentration, has a decreasing trend as the column length decreases (Fig. 3a).

Putting all the above results together, it becomes clear that the optimal column length leading to the highest SMB throughput occurs at the boundary between the pressure-drop limiting region and the raffinate-concentration limiting region.

In the Case I optimization performed so far, the lower limit in $C_{raf,A}/C_{feed,A}$ has been set at 0.9. It will be interesting to examine

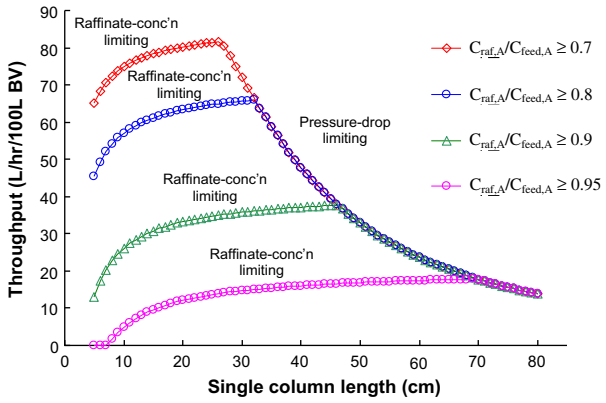

Fig. 4. Effect of the $C_{raf,A}/C_{feed,A}$ limit on the results from the Case I optimization with the constraint on the raffinate product concentration.

how the magnitude of the $C_{raf,A}/C_{feed,A}$ limit affects the optimization results. For this task, additional optimizations were carried out while varying the magnitude of the $C_{raf,A}/C_{feed,A}$ limit, and the results are presented in Fig. 4. One of the noteworthy observations is that the maximum throughput obtainable becomes lower as the $C_{raf,A}/C_{feed,A}$ limit is set higher. This indicates that throughput and product concentration, in fact, are of conflicting nature in the stage of SMB design. Another noteworthy phenomenon is that the optimal column length leading to the maximum throughput increases with enlarging the magnitude of the $C_{raf,A}/C_{feed,A}$ limit. This phenomenon is in consistent with the previous statement that the use of a larger column length is effective in decreasing the *RD*-factors $(\Delta_A^{II}, \Delta_A^{IV})$ and thus increasing the raffinate product concentration.

4.2. Case I optimization with the constraint on the extract product concentration

In this section, the Case I optimization for the SMB of interest was performed under a given constraint on the extract product concentration while all the other optimization conditions were kept the same as in the previous section. This task was repeated by varying the column length at the intervals of 1 cm, which was then carried out several times further while changing the lower limit in $C_{ext,B}/C_{feed,B}$. The results from such a series of optimization tasks are presented in Fig. 5.

It is readily seen that the overall trends in the effects of column length and $C_{ext,B}/C_{feed,B}$ limit on the throughput in Fig. 5 is similar to those from the previous Case I optimization with the $C_{raf,A}/C_{feed,A}$ limit. First, it is confirmed from Fig. 5 that there exists an optimal column length leading to the maximum throughput, where in the region of longer column lengths than the optimal one, the throughput was limited by the pressure-drop constraint whereas in the region of shorter column lengths than the optimal one, the throughput was limited by the constraint on the extract product concentration.

In addition, Fig. 5 shows that the optimal column length leading to the maximum throughput increases as the $C_{ext,B}/C_{feed,B}$ limit is set higher. The occurrence of such phenomenon is due to the fact that the factors promoting the extract product dilution, i.e. the *ED*-factors $(\Delta_B^{I}, \Delta_B^{III})$ can be reduced by increasing the column length, which can be grasped by their relevant expressions from the SWD (Eqs. (3) and (6)).

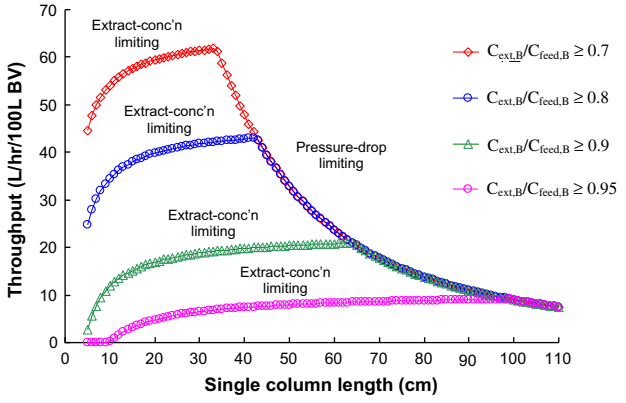

Fig. 5. Effect of the $C_{ext,B}/C_{feed,B}$ limit on the results from the Case I optimization with the constraint on the extract product concentration.

4.3. Case II optimization with the constraint on the raffinate product concentration

In the above Case I optimization, the column configuration was fixed at 2–2–2–2. It will be a worthwhile task to investigate how the optimization of the SMB with the constraint on the product concentration is affected by the column configuration. For this task, the Case II optimization, where the column configuration was included as one of the decision variables, was performed in this section.

In the first place, the Case II optimization with the constraint of $C_{raf,A}/C_{feed,A} \geqslant 0.9$ was carried out while varying the total column length. The throughputs resulting from such Case II optimization and those from the previous Case I optimization with the same constraint were then compared in Fig. 6 while keeping the total column length the same between the two cases. Note that the throughputs from the Case II optimization surpass those from the Case I optimization over the entire range of total column length. Particularly, it is worth noting that the extent of the throughput improvement from the Case II optimization is more pronounced in the raffinate-concentration limiting region than in the pressure-drop limiting region. This result indicates that the column configuration can play an important role in the optimization of the SMB with the constraint on product concentration.

To find out a clue to the reason for the aforementioned phenomenon, it is necessary to check the column configuration of the SMB from the Case II optimization, particularly in the raffinate-concentration limiting region. The information on such column configuration is marked on top of the relevant throughput data points in Fig. 6. It is worth noting first that the SMB from the Case II optimization has a larger number of columns in zones II and

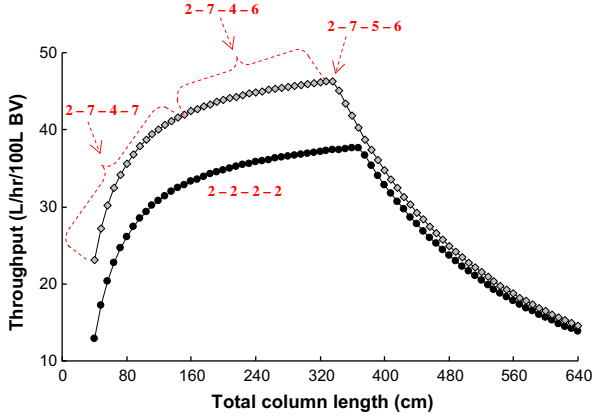

Fig. 6. Comparison of the results from the Case I and II optimizations with the same constraint of $C_{raf,A}/C_{feed,A} \geqslant 0.9$. The black and gray symbols indicate the results from the Case I and Case II optimizations respectively.

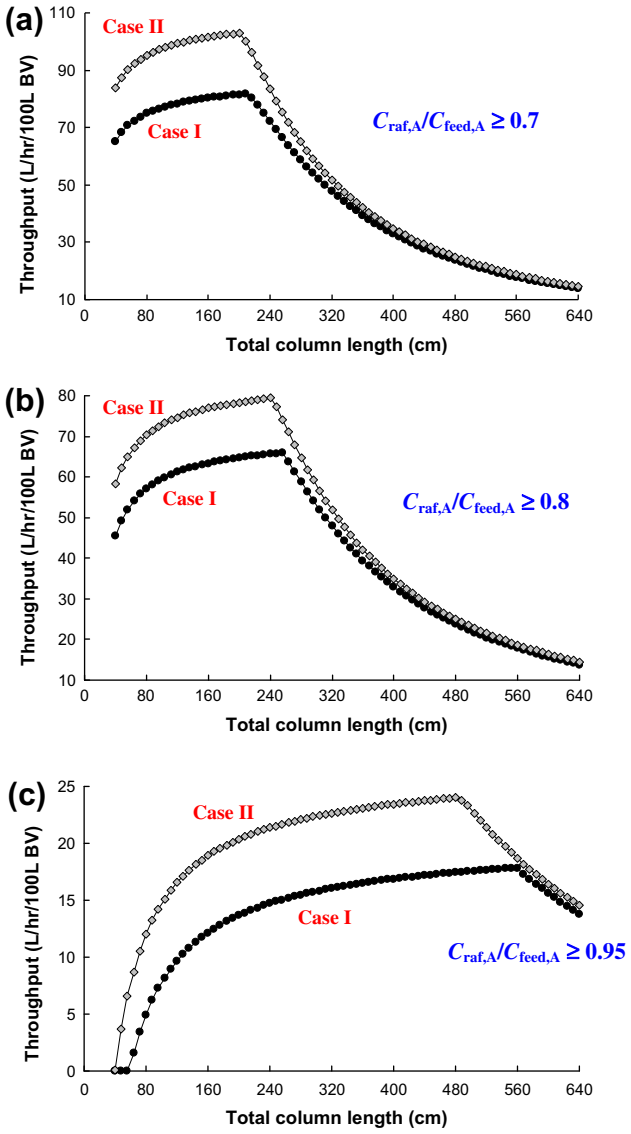

Fig. 7. Comparison of the additional results from the Case I and II optimizations with the same constraint of $C_{raf,A}/C_{feed,A}$. (a) $C_{raf,A}/C_{feed,A} \geq 0.7$, (b) $C_{raf,A}/C_{feed,A} \geq 0.8$, (c) $C_{raf,A}/C_{feed,A} \geq 0.95$. The black and gray symbols indicate the results from the Case I and Case II optimizations respectively.

IV, compared to the SMB from the Case I optimization where the column configuration was fixed at 2–2–2–2. According to the *RD*-factors ($\Delta_A^{II}, \Delta_A^{IV}$), the use of more columns in zones II and IV promotes an increase in the raffinate concentration. It is thus evident that the SMB from the Case II optimization is more favorable for attaining the target level of the raffinate concentration than the SMB from the Case I optimization. In addition to such advantage, it is worth mentioning that the SMB from the Case II optimization have more columns in the separation zones (II and III), compared to that from the Case I optimization. This is also of help to the attainment of higher feed flow rate according to the literature [22]. Due to the aforementioned two factors, the SMB with the optimal column configuration leads to higher throughput than that of the SMB with the fixed column configuration, particularly in the region where the throughput is limited by the constraint on the raffinate product concentration. This result indicates the importance of selecting a proper column configuration in the stage of optimizing the SMB with the constraint on the product concentration.

In the Case II optimization performed so far, the lower limit in $C_{raf,A}/C_{feed,A}$ has been set at 0.9. To investigate the effect of the $C_{raf,A}/C_{feed,A}$ limit on the optimization results, additional Case II optimizations were carried out while varying the magnitude of the $C_{raf,A}/C_{feed,A}$ limit. The resulting throughputs from these tasks were then compared in Fig. 7 with those from the Case I optimizations having the same constraints on the raffinate concentration. It is clearly confirmed that the SMB from the Case II optimization outperforms that from the Case I optimization regardless of the $C_{raf,A}/C_{feed,A}$ limit.

To derive another important point, the optimal column configuration leading to the maximum throughput in each of the Case II optimization results is compared in Table 2. It is readily seen that as the $C_{raf,A}/C_{feed,A}$ limit is set higher, zone IV has an increasing number of columns, which is accompanied by a decrease in the number of columns in zone III (N^{III}). By contrast, there is almost no change in the number of columns in zone II (N^{II}). The reason for such trend can also be explained by using the *RD*-factors. As the $C_{raf,A}/C_{feed,A}$ limit is set higher, the column configuration in favor of attaining higher raffinate concentration will be preferred, which will cause N^{II} and/or N^{IV} to be increased according to the *RD*-factor expressions. Between these two, the N^{IV} has more dominating effect on the raffinate concentration than the N^{II} as mentioned in the theory section. For this reason, the enlargement of the $C_{raf,A}/C_{feed,A}$ limit brings about an increase in the N^{IV} while preventing the decrease of the N^{II}. Under such circumstances, it is obvious that the increased columns in zone IV should not come from zone II but from zone III. This means that the N^{III} should be decreased with increasing the magnitude of the $C_{raf,A}/C_{feed,A}$ limit, as can be seen in Table 2.

4.4. Case II optimization with the constraint on the extract product concentration

In this section, the Case II optimization was performed under the constraint on the extract product concentration while keeping all the other conditions the same as in the previous section. The results from such Case II optimization and those from the Case I optimization with the same constraint were then compared in Fig. 8. Like in the previous section, one can clearly see that the throughputs from the Case II optimization with the $C_{ext,B}/C_{feed,B}$ limit are higher in the entire region of total column length, compared to those from the relevant Case I optimization.

To elucidate the reason for the above-mentioned phenomenon, it is worth examining how the columns are assigned to each of the four zones in the SMB from the Case II optimization. For such an examination, the optimal column configuration leading the

Table 2
The optimal column configuration leading to the maximum throughput for each of the Case II optimizations that were performed while varying the magnitude of the $C_{raf,A}/C_{feed,A}$ limit or the $C_{ext,B}/C_{feed,B}$ limit.

Constraint imposed on raffinate concentration		Constraint imposed on extract concentration	
$C_{raf,A}/C_{feed,A}$ limit	Optimal configuration	$C_{ext,B}/C_{feed,B}$ limit	Optimal configuration
0.7	2–7–7–4	0.7	6–4–8–2
0.8	2–7–6–5	0.8	6–4–8–2
0.9	2–7–5–6	0.9	7–3–8–2
0.95	2–8–3–7	0.95	8–2–8–2

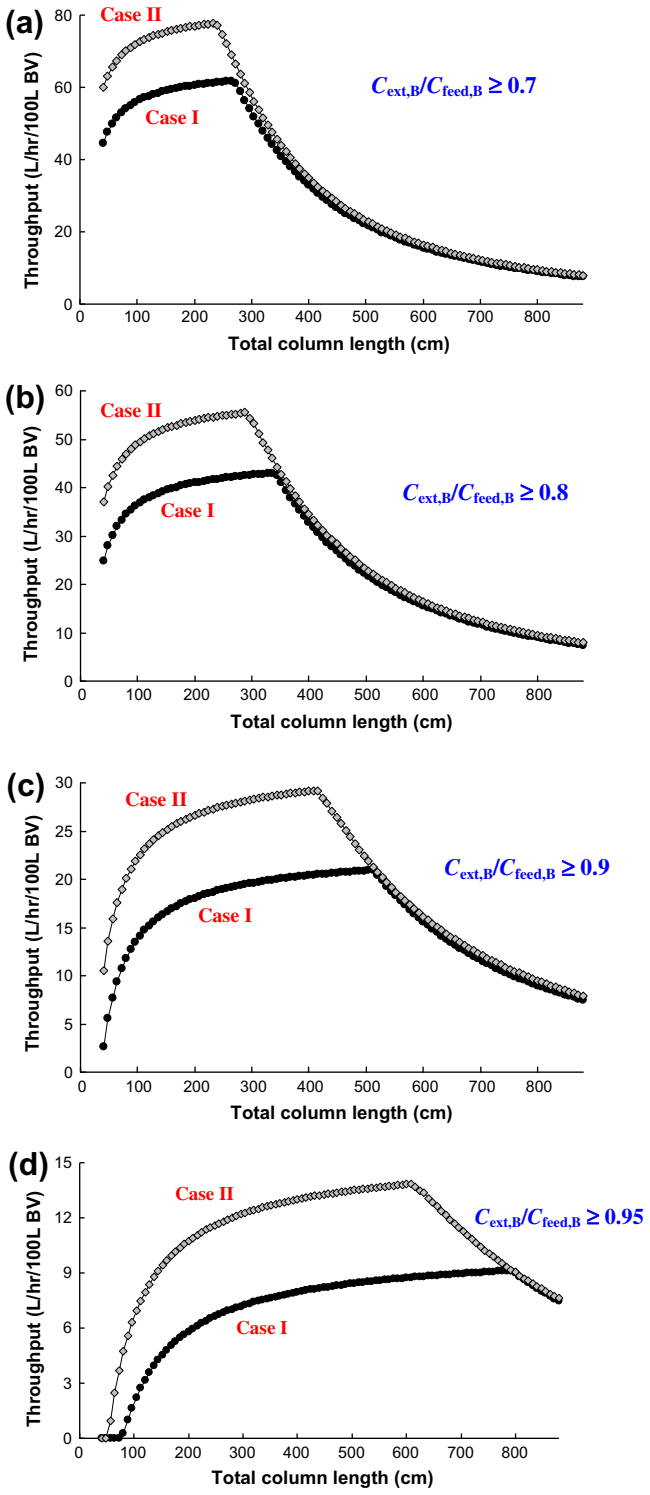

Fig. 8. Comparison of the additional results from the Case I and II optimizations with the same constraint of $C_{ext,B}/C_{feed,B}$. (a) $C_{ext,B}/C_{feed,B} \geq 0.7$, (b) $C_{ext,B}/C_{feed,B} \geq 0.8$, (c) $C_{ext,B}/C_{feed,B} \geq 0.9$, (d) $C_{ext,B}/C_{feed,B} \geq 0.95$. The black and gray symbols indicate the results from the Case I and Case II optimizations respectively.

maximum throughput is presented in Table 2 with respect to the magnitude of the $C_{ext,B}/C_{feed,B}$ limit. It is readily observed that the columns are assigned to each of the four zones in favor of higher extract concentration and/or higher feed flow rate than the 2–2–2–2 configuration. This point can readily be understood by utilizing (1) the relationship between the *ED*-factors and the number of columns in zones I and III and (2) the relationship between the feed flow rate and the number of columns in the separation zones (II and III).

Such two relationships can also be utilized in explaining why the enlargement of the $C_{ext,B}/C_{feed,B}$ limit leads to an increase in the N^{I} and a decrease in the N^{II} as seen in Table 2. This is mostly because more emphasis must be placed on the increase of the extract concentration if the $C_{ext,B}/C_{feed,B}$ limit is set higher. In other words, a portion of the columns in zone II should be re-assigned in such a way that the number of columns in zone I can be increased, for the purpose of increasing the extract concentration at the expense of some throughput. All of these results indicate that the optimization of the column configuration is essential in the stage of developing an SMB process with the constraint on product concentration.

5. Conclusions

A four-zone SMB process for separation of the binary amino acid mixture, which was available in the literature, was optimized to maximize throughput under the given constraints on product concentration and pressure drop. This task was assisted by the SMB optimization tool that was prepared on the basis of the standing wave design (SWD) method. The results showed that column length played an important role in the optimization of the SMB with the constraint on product concentration. It was found first that an increase in the column length led to higher throughput in the region of short columns, where the throughput was limited by the constraint on the product concentration. In the other region of long columns where the throughput was limited by the pressure-drop constraint, the throughput showed a decreasing trend as the column length increased. As a result, the optimal column length leading to the highest throughput occurred at the boundary between the product-concentration limiting region and the pressure-drop limiting region. In addition to the column length, the column configuration was also found to have a considerable effect on the throughput and the production concentration. As the target level of the raffinate product concentration was set higher, the allocation of more columns to zone IV was favorable for obtaining the maximum throughput. By contrast, as the target level of the extract product concentration was set higher, the allocation of more columns to zone I was favorable for obtaining the maximum throughput. All of the results in this study will be of help to the optimal design of an SMB process with a strict requirement on the level of product concentration.

Acknowledgments

This research was supported by Basic Science Research Program through the National Research Foundation of Korea (NRF) funded by the Ministry of Education, Science and Technology (Grant Number 2012R1A2A2A01019790). Also, it was partially supported by the Manpower Development Program for Energy & Resources supported by the Ministry of Knowledge and Economy (MKE), Republic of Korea.

Appendix A. Derivation of two dimensionless product concentrations ($\overline{C}_{raf,A}$ and $\overline{C}_{ext,B}$) from the SWD equations

Using the material balance on component A, the following equation can be obtained.

$$Q_{raf}C_{raf,A} = Y_A Q_{feed} C_{feed,A} \quad \text{(A1)}$$

Since $Q_{feed} = Q^{III} - Q^{II}$ and $Q_{raf} = Q^{III} - Q^{IV}$, the above equation can be re-expressed as follows.

$$\overline{C}_{raf,A} \equiv \frac{C_{raf,A}}{C_{feed,A}} = Y_A \frac{Q_{feed}}{Q_{raf}} = Y_A \left(\frac{Q^{III} - Q^{II}}{Q^{III} - Q^{IV}} \right) \quad (A2)$$

Substitution of the above Q^j by the relevant SWD equations (Eqs. (1b), (1c), (1d)) results in

$$\overline{C}_{raf,A} \equiv \frac{C_{raf,A}}{C_{feed,A}} = Y_A \left(\frac{S(1-\varepsilon_b)(\delta_B - \delta_A)v - \Delta_B^{III} - \Delta_A^{II}}{S(1-\varepsilon_b)(\delta_B - \delta_A)v - \Delta_B^{III} + \Delta_A^{IV}} \right) = Y_A \left(\frac{\psi - \Delta_A^{II}}{\psi + \Delta_A^{IV}} \right) \quad (A3)$$

where $\psi = S(1-\varepsilon_b)(\delta_B - \delta_A)v - \Delta_B^{III}$.

Using the same procedures as above, the expression for $\overline{C}_{ext,B}$ can be derived from the SWD equations in the following manner.

$$Q_{ext} C_{ext,B} = Y_B Q_{feed} C_{feed,B} \quad (A4)$$

$$\overline{C}_{ext,B} \equiv \frac{C_{ext,B}}{C_{feed,B}} = Y_B \frac{Q_{feed}}{Q_{ext}} = Y_B \left(\frac{Q^{III} - Q^{II}}{Q^{I} - Q^{II}} \right) \quad (A5)$$

$$\overline{C}_{ext,B} \equiv \frac{C_{ext,B}}{C_{feed,B}} = Y_A \left(\frac{S(1-\varepsilon_b)(\delta_B - \delta_A)v - \Delta_A^{II} - \Delta_B^{III}}{S(1-\varepsilon_b)(\delta_B - \delta_A)v - \Delta_A^{II} + \Delta_B^{I}} \right) = Y_A \left(\frac{\lambda - \Delta_B^{III}}{\lambda + \Delta_B^{I}} \right) \quad (A6)$$

where $\lambda = S(1-\varepsilon_b)(\delta_B - \delta_A)v - \Delta_A^{II}$.

References

[1] L.S. Pais, J.M. Loureiro, A.E. Rodrigues, Separation of 1,1′-bi-2-naphthol enantiomers by continuous chromatography in simulated moving bed, Chem. Eng. Sci. 52 (1997) 245–257.
[2] Y. Xie, B. Hritzko, C.Y. Chin, N.H.L. Wang, Separation of FTC-ester enantiomers using a simulated moving bed, Ind. Eng. Chem. Res. 42 (2003) 4055–4067.
[3] K.B. Lee, C.Y. Chin, Y. Xie, G.B. Cox, N.H.L. Wang, Standing wave design of a simulated moving bed under a pressure limit for enantioseparation of phenylpropanolamine, Ind. Eng. Chem. Res. 44 (2005) 3249–3267.
[4] S.H. Kang, J.H. Kim, S. Mun, Optimal design of a tandem simulated moving bed process for separation of paclitaxel, 13-dehydroxybaccatin III, and 10-deacetylpaclitaxel, Process Biochem. 45 (2010) 1468–1476.
[5] J.S. Park, W.S. Kim, J.M. Kim, I.H. Kim, Ibuprofen racemate separation by simulated moving bed, J. Chem. Eng. Jpn. 41 (2008) 624–626.
[6] M. Minceva, P.S. Gomes, V. Meshko, A.E. Rodrigues, Simulated moving bed reactor for isomerization and separation of p-xylene, Chem. Eng. J. 140 (2008) 305–323.
[7] K. Hasegawa, Y. Okamoto, T. Nakamura, T. Kaneko, C. Sano, K. Iitani, Method for Purifying Branched Chain Amino Acids, U.S. Patent, 6072083, 2000.
[8] M.A. Cremasco, B.J. Hritzko, Y. Xie, N.H.L. Wang, Parameter estimation for amino acids adsorption in a fixed bed by moment analysis, Braz. J. Chem. Eng. 18 (2001) 181–194.
[9] Z. Ma, N.H.L. Wang, Standing wave analysis of SMB chromatography: linear systems, AIChE J. 43 (1997) 2488–2508.
[10] K.B. Lee, R.B. Kasat, G.B. Cox, N.H.L. Wang, Simulated moving bed multiobjective optimization using standing wave design and genetic algorithm, AIChE J. 54 (2008) 2852–2871.
[11] B.J. Hritzko, Y. Xie, R. Wooley, N.H.L. Wang, Standing wave design of tandem SMB for linear multicomponent systems, AIChE J. 48 (2002) 2769–2787.
[12] H.G. Nam, S.H. Jo, S. Mun, Comparison of Amberchrom-CG161C and Dowex99 as the adsorbent of a four-zone simulated moving bed process for removal of acetic acid from biomass hydrolyzate, Process Biochem. 46 (2011) 2044–2053.
[13] G. Storti, M. Masi, S. Carra, M. Morbidelli, Optimal design of multicomponent countercurrent adsorption separation processes involving nonlinear equilibria, Chem. Eng. Sci. 44 (1989) 1329–1345.
[14] D.C.S. Azevedo, A.E. Rodrigues, Design of a simulated moving bed in the presence of mass transfer resistances, AIChE J. 45 (1999) 956–966.
[15] A.E. Rodrigues, L.S. Pais, The design of SMB chiral separation using the concept of separation volume, Sep. Sci. Technol. 39 (2004) 245–270.
[16] V.M.T. Silva, M. Minceva, A.E. Rodrigues, Novel analytical solution for a simulated moving bed in the presence of mass-transfer resistance, Ind. Eng. Chem. Res. 43 (2004) 4494–4502.
[17] J.S. Hur, P.C. Wankat, New design of simulated moving bed for ternary separations, Ind. Eng. Chem. Res. 44 (2005) 1906–1913.
[18] Y. Kawajiri, L.T. Biegler, Nonlinear programming superstructure for optimal dynamic operations of simulated moving bed processes, Ind. Eng. Chem. Res. 45 (2006) 8503–8513.
[19] S. Ergun, Flow through packed columns, Chem. Eng. Prog. 48 (1952) 89–94.
[20] S.F. Chung, C.Y. Wen, Longitudinal dispersion of liquid flowing through fixed and fluidized beds, AIChE J. 14 (1968) 857–866.
[21] E.J. Wilson, C.J. Geankoplis, Liquid mass transfer at very low Reynolds numbers in packed beds, Ind. Eng. Chem. Fundam. 5 (1966) 9–14.
[22] K.B. Lee, S. Mun, F. Cauley, G.B. Cox, N.H.L. Wang, Optimal standing wave design of nonlinear simulated moving bed systems for enantioseparation, Ind. Eng. Chem. Res. 45 (2006) 739–752.